

# Mode of Complex Formation Between Thiones and Silver Ion Within a Photothermographic Formulation: The Crystal and Molecular Structure of Hexa-(silver-5-methyl-2-mercaptobenzimidazole THF)<sup>1</sup>

D. R. Whitcomb<sup>▲</sup>

Carestream Health, Inc., 1 Imation Way, Oakdale, Minnesota 55129

E-mail: david.whitcomb@carestreamhealth.com

Richard P. Swatloski and Robin D. Rogers

Department of Chemistry, Center for Green Chemistry, The University of Alabama,

Tuscaloosa, Alabama 35487

**Abstract.** The reaction of 5-methyl-2-mercaptobenzimidazole (5MBI) with silver ions in organic solvents form widely varying macrostructured or polymeric structures, depending on the anion type. In the case of carboxylate anions, the reaction of 5MBI with  $[\text{Ag}(\text{O}_2\text{C}_x\text{H}_{2x-1})]_2$  results in high yields of hexameric clusters containing bridging 5MBI units,  $[\text{Ag}\cdot 5\text{MBI}\cdot\text{THF}]_6$ , the details of which are reported here. The six silver atoms of  $[\text{Ag}\cdot 5\text{MBI}]_6$  are arranged as a trigonal antiprism with each 5MBI bonded to three silver atoms, two bridged with the sulfur and the third bridged with the nitrogen. From these results, and comparison to the reaction of AgBr that forms a polymeric  $[\text{AgBr}\cdot\text{MBI}(\text{acetone})_{0.5}]_4$  complex, a mixture of different complexes may be expected to form in a photothermographic imaging construction. © 2007 Society for Imaging Science and Technology.

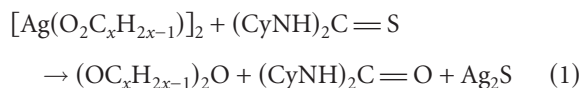
[DOI: 10.2352/J.ImagingSci.Technol.(2007)51:6(547)]

## INTRODUCTION

Methyl-2-mercaptobenzimidazole (MBI, representing the 4- and 5-methyl isomers, and the parent 2-mercaptobenzimidazole) and its analogs have been used extensively in conventional photographic imaging materials. MBI properties include antifoggant,<sup>1–6</sup> shelf stability,<sup>7</sup> and print stabilization.<sup>8,9</sup> In addition, MBI has been found to be an important component in photothermographic imaging materials, which are light exposed but thermally developed without conventional wet processing.<sup>10–12</sup> We reported the solid state structure of the  $[\text{AgBr}\cdot\text{MBI}\cdot(\text{acetone})_{0.5}]_4$  complex that is formed in organic solvent from MBI and the light sensitive component of photographic and photothermographic films.<sup>13</sup> Under those conditions, despite the labile proton available on the MBI, the ligand acts

as a neutral donor, unlike its adsorption to silver halide surfaces in aqueous conditions. In this latter case, as demonstrated by electron spectroscopy for chemical analysis (ESCA) and x-ray appearance near-edge structure (XANES) spectroscopies,<sup>14,15</sup> MBI coordination occurs through the deprotonated thiol sulfur. The AgMBI complex and, apparently, HBr are the result of this complex formation process.

As noted previously,<sup>13</sup> the coordination behavior of MBI might be considered to be similar to that of thioureas since MBI is essentially a thiourea derivative. It is known, however, that the reaction of thioureas with silver carboxylates, such as silver benzoate, acetate, phthalate, propionate and succinate, in organic media very efficiently produces Ag<sub>2</sub>S and the corresponding anhydride and carbodiimide,<sup>16</sup> as illustrated by the reaction of silver carboxylates and 1,2-dicyclohexylthiourea,  $(\text{CyNH})_2\text{C}=\text{S}$ , in the following equation:



We have found that the same reaction occurs with long chain length silver carboxylates, such as those found in a typical photothermographic construction,<sup>10–12</sup> albeit to a more limited extent. The Ag<sub>2</sub>S appears in all cases, but the yield is substantially different with some apparent relationship to the chain length. Therefore, the coordination chemistry implications for incorporating MBI into solvent based photothermographic formulations can be complicated: In the presence of AgBr,  $[\text{AgBr}\cdot\text{MBI}(\text{acetone})_{0.5}]_4$  would be expected, but in the presence of silver carboxylates, Ag<sub>2</sub>S. However, we have found that instead of Ag<sub>2</sub>S, a new stable hexameric silver cluster is formed from the reaction of the silver carboxylates with MBI. Characterizing both AgMBI products should be useful for better understanding the coordination chemistry of MBI in those formulations. The difference in the products formed, a polymeric tetramer compared to a hexamer, respectively, can be directly attributed to

<sup>▲</sup>IS&T Member

<sup>1</sup>CCDC 273242 contains the supplementary crystallographic data for this paper. These data can be obtained free of charge via [www.ccdc.cam.ac.uk/data-request/cif](http://www.ccdc.cam.ac.uk/data-request/cif), by e-mailing [data-request@ccdc.cam.ac.uk](mailto:data-request@ccdc.cam.ac.uk), or by contacting The Cambridge Crystallographic Data Centre, 12 Union Road, Cambridge CB2 1EZ, UK; fax: +44(0)1223-336033.

Received Jul. 6, 2007; accepted for publication Jul. 26, 2007.

1062-3701/2007/51(6)/547/5/\$20.00.

the counterion, and the corresponding conjugate base strength, of the carboxylate versus halide. The results of the formation of the  $[\text{Ag}\cdot 5\text{MBI}]_6$  complex formed from the silver carboxylate starting material and its solid-state structure are discussed below.

## EXPERIMENTAL

Preparation of  $[\text{Ag}\cdot 5\text{MBI}]_6$  was carried out by mixing stoichiometric amounts of the silver carboxylate (normally silver stearate, but other alkyl chain lengths produce the same result) and 5MBI in THF. The 5MBI deprotonation reaction is rapid, and quantitatively forms a bright yellow solution (completely clear) that soon begins to deposit the yellow  $[\text{Ag}\cdot 5\text{MBI}\cdot\text{THF}]_6$  complex. Standing for extended times (several weeks at room temperature, or days at 3°C), the yellow solution eventually becomes virtually colorless, as a mixture of sizes and quality of clear yellow crystals form. The self-assembly of the  $\text{Ag}_65\text{MBI}_6$  during this process, including alternating N–H hydrogen bond donors above and below the triangular faces of the  $\text{Ag}_6$  antiprism and the layer-like packing, leads to the crystallization of loosely held solvates. Generally, the amount of occluded solvent is variable, and the crystal quality for x-ray diffraction investigation is usually poor. Nevertheless, after four data sets, crystals containing a stoichiometric amount of THF were isolated and the structural characterization proceeded smoothly. Elemental analysis of this last complex (Galbraith Laboratories) was satisfactory for  $[\text{Ag}\cdot 5\text{MBI}\cdot\text{THF}]_6$ . Thermogravimetric analysis (TGA) (TA Instruments, Model 951, heating rate of 10°C/min under a nitrogen purge at approximately 50 mL/min) revealed loss of THF [room temperature (RT)–110°C; 21.5%, theory=20.9%], 5MBI-S (300°C–370°C; 35.8%, theory=38.4%), and residual  $\text{Ag}_2\text{S}$  above 400°C (40.6%, theory=36.0%).

Single crystals, cooled to –100°C during data collection, were mounted on a fiber and transferred to the goniometer of a Siemens SMART diffractometer equipped with Mo  $K\alpha$  radiation ( $\lambda=0.71073$  Å) and a charge coupled device (CCD) area detector. The SHELXTL software, version 5, was used for solutions and refinements.<sup>17</sup> Absorption corrections were made with SADABS.<sup>18</sup> Each structure was refined by full-matrix least squares on  $F^2$ . A summary of data collection parameters is given in Table I. All four data sets collected indicated the same approximate unit cell with systematic absences and statistics indicating the correct space group as  $R\text{-}3c$ . In each case, the location of the  $\text{Ag}_65\text{MBI}_6$  core was readily apparent; however, the data quality suffered greatly because of lost solvent or extra solvent and unresolvable electron density in the solvent positions.

The three preliminary data sets refined revealed slightly varying solvent features of the crystallization and packing of the title compound. The first was formulated as  $[\text{Ag}\cdot 5\text{MBI}\cdot\text{THF}]_6\cdot\text{THF}$ , had a unit cell volume of 11,957.92 Å<sup>3</sup>, and refined to  $R1=4.46\%$ . The hydrogen bonded THF site and the free THF site exhibited total unresolvable disorder. A second data set with this same formulation was studied, however, the unit cell volume was

**Table I.** Crystallographic data for  $[\text{Ag}\cdot 5\text{MBI}\cdot\text{THF}]_6$ .

Empirical formula	$\text{C}_{66}\text{H}_{78}\text{Ag}_6\text{N}_{12}\text{O}_6\text{S}_6$
Formula weight	1974.98
Radiation/wavelength	Mo $K\alpha$ (graphite monochromator)/0.71073 Å
Temperature	173(2) K
Space group	$R\text{-}3c$ (No. 167)
Unit cell dimensions	$a=16.6542(2)$ Å; $\alpha=90^\circ$ $b=16.6542(2)$ Å; $\beta=90^\circ$ $c=47.2790(13)$ Å; $\gamma=120^\circ$
Volume	11356.5(4) Å <sup>3</sup>
Z	6
Density (calculated)	1.733 Mg/m <sup>3</sup>
Absorption coefficient	1.743 mm <sup>-1</sup>
Final $R$ indices $[I > 2\sigma(I)]^a$	$R1=0.0368$ , $wR2=0.0995$
$R$ indices (all data) <sup>a</sup>	$R1=0.0467$ , $wR2=0.1159$

$$^a R1 = \frac{\sum ||F_o| - |F_c||}{\sum |F_o|}; wR2 = \left\{ \frac{\sum w(F_o^2 - F_c^2)^2}{\sum w(F_o^2)} \right\}^{1/2}.$$

larger at 12,575.53 Å<sup>3</sup> ( $R1=7.50\%$ ) and the 5-methyl substituent in the ligand was found to be disordered. High thermal motion was noted in the  $\text{Ag}_6\text{S}_6\text{N}_6$  core. The third data set was formulated as  $[\text{Ag}\cdot 5\text{MBI}\cdot\text{THF}]_6\cdot 0.5\text{H}_2\text{O}$  (volume=11,037.68 Å<sup>3</sup>;  $R1=6.82\%$ ) with water molecules hydrogen bonded to each  $\text{S}_3$  triangular face.

In the fourth data set collected, data quality was much better and during the solution and refinement stages the THF sites appeared to be fully occupied. The THF molecules in the final refinement still exhibit high thermal motion, however, this is not usual for THF solvates even at reduced temperatures. All nonhydrogen atoms were refined with anisotropic thermal parameters, then the hydrogen atom bonded to  $\text{N}_2$  was located from a difference Fourier map and allowed to ride on  $\text{N}_2$  at a fixed distance. All other hydrogen atoms were placed in calculated positions and allowed to ride on the bonded atom. All hydrogen atoms were refined with isotropic thermal parameters  $U(H)=1.2 \cdot U_{\text{eq}}(\text{C or N})$ .

## RESULTS AND DISCUSSION

The tautomerism of 5MBI is analogous to the 2-mercapto-benzothiazole equilibrium,<sup>19</sup> thus, the 5MBI structure should favor the thione form. The thiol form, on the other hand, was found to be favored for cyclic thioureas in the chemical ripening processes of silver halide microcrystals.<sup>20</sup>

The reaction of 5MBI with  $\text{AgBr}$  and  $[\text{Ag}(\text{O}_2\text{CCH}_3)]_2$  proceeds extremely rapidly and quantitatively at RT in organic solvents, particularly in acetone and THF. In the case of  $\text{AgBr}$ , a white slightly soluble and very light stable complex having the stoichiometry  $[\text{AgBr}\cdot\text{MBI}(\text{acetone})_{0.5}]_4$  is produced.<sup>15</sup> With  $[\text{Ag}(\text{O}_2\text{CCH}_3)]_2$  a bright yellow initially very soluble (in THF) and very light stable complex results.

The silver atoms within the  $[\text{Ag}(\text{O}_2\text{CR})]_2$  normally used in photothermographic formulations are all three-coordinate due to the bonding interaction between adjacent silver

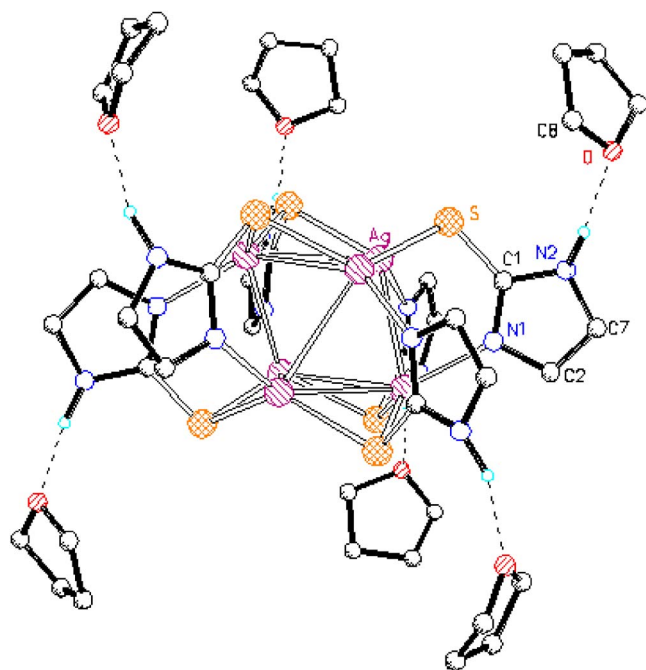


Figure 1. The formula unit for  $[\text{Ag}\cdot 5\text{MBI}\cdot \text{THF}]_6$  (most hydrogen atoms and the benzosubstituent removed for clarity).

dimers, as described previously.<sup>21</sup> The silver atoms at the solid surface, the (100) and (010) planes, however, are only two-coordinate. Consequently, these surface silver atoms are readily available for reaction with suitable ligands. In the case of 5MBI, the thione sulfur can be envisioned to coordinate first with a silver ion in the silver carboxylate dimer on the surface of the  $[\text{Ag}(\text{O}_2\text{CR})_2]$  crystal during the formulation of a photothermographic emulsion. The first step of 5MBI solubilization of  $[\text{Ag}(\text{O}_2\text{CR})_2]$  probably produces an asymmetric silver complex intermediate, such as “[5MBI·Ag<sub>2</sub>·O<sub>2</sub>CR]” (which we were unable to isolate). This composition is similar to those described earlier, and although asymmetric silver carboxylate complexes are not well known, there is precedence.<sup>13,22,23</sup> The addition of a second MBI ligand to the soluble “[5MBI·Ag<sub>2</sub>·O<sub>2</sub>CR]” intermediate could then readily eliminate the second carboxylic acid, followed by self-assembly, leading to the  $[\text{Ag}\cdot 5\text{MBI}]_6$  complex obtained.

#### Structure Determination of $[\text{Ag}\cdot 5\text{MBI}\cdot \text{THF}]_6$

The formula unit for the title compound is shown in Figure 1. The  $[\text{Ag}\cdot 5\text{MBI}]_6$  core contains 12 bridging Ag–thione and 6 Ag–N<sub>deprotonated</sub> bonds forming a discrete entity unlike the polymeric structure observed for the AgBr complex.

The six silver atoms of  $[\text{Ag}\cdot 5\text{MBI}]_6$  are arranged as a trigonal antiprism. Each 5MBI is bonded to three silver atoms; two that are bridged with the sulfur and the third with the nitrogen. The 5MBI S and N atoms alternate spatially, either “up” to match the silver triangle above or “down” to align with the silver triangle below. This produces two effects. First, the S atoms form their own trigonal antiprism with the faces displaced above or below those of the Ag atoms. Second, the N2 positions direct three hydrogen bond

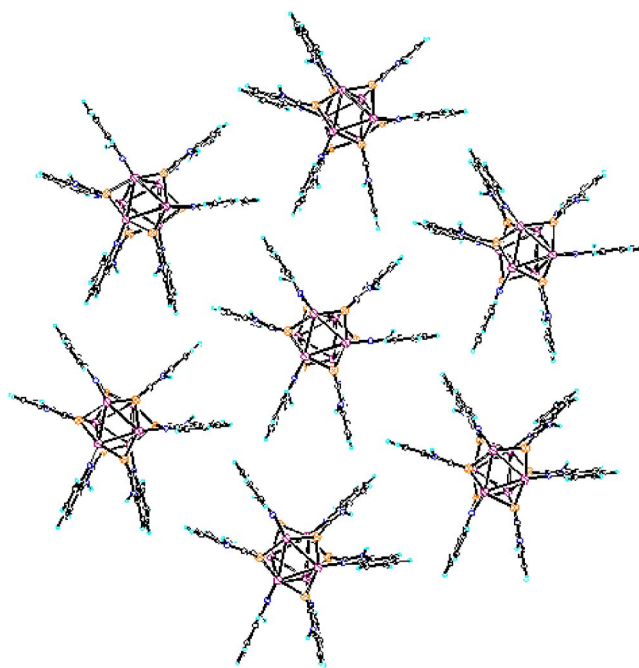


Figure 2. 2D packing of  $[\text{Ag}\cdot 5\text{MBI}\cdot \text{THF}]_6$  rotors.

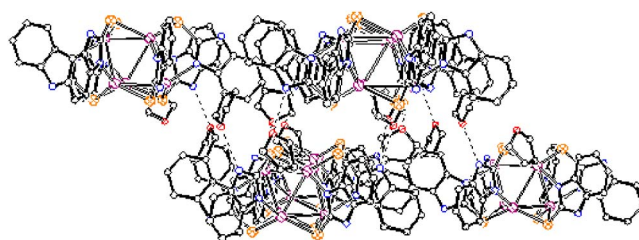


Figure 3. Packing of  $[\text{Ag}\cdot 5\text{MBI}\cdot \text{THF}]_6$  layers.

donating sites above and three below the triangular faces. These hydrogen atoms are each hydrogen bonded to the oxygen atom ( $\text{H}\cdots\text{O}=1.805\text{ \AA}$ ;  $\text{N}(2)\text{—H}\cdots\text{O}=159^\circ$ ) of a THF molecule and are responsible for the observed hexasolvation.

The structure exhibits supramolecular weak intermolecular hydrogen bond features. The  $[\text{Ag}\cdot 5\text{MBI}]_6$  crystallizes with the 5MBI planes essentially parallel forming an approximate rotor. It is interesting to note, however, that the interplanar separations are not equivalent as measured by the two unique N–Ag $\cdots$ Ag–N torsion angles of  $98.3^\circ$  and  $69.6^\circ$  to neighboring 5MBI molecules. This allows the “rotors” to pack in two-dimensional (2D) layers (via edge-to-face aromatic stacking in the *ab* unit cell plane), which resemble locked gears, as seen in Figure 2. The two 5MBI ligands that are closer together fit between the two ligands that are farther apart in a neighboring molecule. The closest approach in these interactions is the edge on contact  $\text{C}(5)\text{—H}(5)\cdots\text{C}(5)^*=160.8^\circ$ ;  $\text{H}(5)\cdots\text{C}(5)^*=3.045\text{ \AA}$ .

The packing of the 2D layers in the unit cell *c* direction, as seen in Figure 3, appears to be controlled by an edge (of the 5MBI)-to-S interaction. The pertinent distance and angle are  $\text{C4—H4}\cdots\text{S}=151^\circ$  and  $\text{H4}\cdots\text{S}=3.158\text{ \AA}$ . The 2D

**Table II.** Selected bond lengths [Å] and angles [°] for [Ag·5MBI·THF]<sub>6</sub>

Bond Distances	
Ag–N(1)#1	2.242(5)
Ag–S	2.458(2)
Ag–S#2	2.534(2)
S–C(1)	1.727(6)
N(1)–C(1)	1.329(7)
N(1)–C(2)	1.394(8)
N(2)–C(1)	1.377(8)
N(2)–C(7)	1.387(8)
Ag···Ag#1	3.0983(8)
Ag···Ag#2	3.1425(8)
Bond Angles	
N(1)#1–Ag–S	125.50(12)
N(1)#1–Ag–S#2	102.21(12)
S–Ag–S#2	124.77(7)
C(1)–S–Ag	102.7(2)
C(1)–S–Ag#3	100.0(2)
Ag–S–Ag#3	78.00(5)
C(11)–O–C(8)	107.4(7)
C(1)–N(1)–C(2)	106.4(5)
C(1)–N(1)–Ag#1	128.8(4)
C(2)–N(1)–Ag#1	124.5(4)
C(1)–N(2)–C(7)	107.7(5)

Symmetry transformations used to generate equivalent atoms: #1  $y+1/3, x-1/3, -z+1/6$ ; #2  $-x+y+1, -x+1, z$ ; #3  $-y+1, x-y, z$ .

sheet motif of engaged rotors is the more efficient packing arrangement and the packing motif of the layers in the *c* direction creates the voids, which the solvent molecules fill. Of the three additional data sets refined in this study, it was the unique *c* axis that exhibited the most variation.

Selected distances and angles for [Ag·5MBI·THF]<sub>6</sub> are given in Table II. The Ag–S bond lengths in the S–Ag–S units from the bridging 5MBI ligand are all 2.458(2) and 2.534(2) Å, while N(1) is coordinated to Ag at an Ag–N separation of 2.242(5) Å.

There are several complexes reported recently in the literature having structural similarities to [Ag·5MBI·THF]<sub>6</sub>. The silver complex of a smaller 1*H*-pyridine-2-thione ligand favors three-dimensional polymeric networks.<sup>24</sup> Silver–silver separations range from 2.959(2) to 3.369(3), bracketing what we observe for the title complex, but longer Ag–N and Ag–S bonds than in [Ag·5MBI·THF]<sub>6</sub>. A second preparation of this complex provided similar, but not identical, features.<sup>25</sup> The silyl derivative of the pyridine thione ligand, 6-*t*-butyldimethylsilyl-2-pyridine-thiol, produces a complex that is also hexameric, which exhibits widely variable Ag···Ag distances, 2.882(3)–4.034(3) Å. As in [Ag·5MBI·THF]<sub>6</sub>, the S bridges two silvers with the aromatic N bound to the Ag below.<sup>26</sup> Similarly, 3 and 3,6-

substituted 2-pyridine-thiols form [AgSR]<sub>6</sub> hexamers, with the same thione two silver bridge overlapping the aromatic N bound to the Ag below. In this case, all Ag···Ag distances are long at 3.323(1) Å.<sup>27</sup>

A related hexamer, also prepared using silver acetate with a chiral (S)-4-isopropylthiazolidine-2-thione ligand, has been reported.<sup>28</sup> This structure is most closely related to the [Ag·5MBI·THF]<sub>6</sub> complexed reported here. The Ag–N, Ag–S, and Ag···Ag distances [two Ag–S at 2.4527(16) and 2.5121(16), one Ag–N at 2.247(5); four Ag···Ag at 2.9811(6), 3.2071(6), 3.3269(8), and 3.2071(6)] all compare well with those seen in the case of [Ag·5MBI·THF]<sub>6</sub> [two Ag–S, 2.458(2) and 2.534(2); one Ag–N, 2.242(5); two Ag···Ag, 3.0983(8) and 3.1425(8)].

Solvated Ag–thiosemicarbazone complexes, [Ag<sub>6</sub>(L1H)<sub>6</sub>](4·DMF·Et<sub>2</sub>O), containing bridging S and N capping groups on hexameric cluster, Ag(1)–N(1), 2.274(4); Ag(1)–S(2), 2.4799(12); Ag(1)–S(3), 2.5107(11) have also been reported. A wide range of Ag···Ag distances were noted, from 2.9358(4) to 3.7202(5) Å.<sup>29</sup>

Finally, the 2-mercaptionicotinic acid ligand also produces a silver hexamer.<sup>30</sup> In this complex, two distorted silver triangles form in which the ligand nitrogens bond the silver in the lower triangle while the sulfur bridges two silver atoms above. The Ag···Ag distances are 2.911(1), 2.924(1), and 3.1129(8), comparable to those observed in [Ag·5MBI·THF]<sub>6</sub> in this study.

## CONCLUSIONS

Both the keto-enol equilibrium forms of 5MBI have now been shown to be incorporated into stable Ag<sup>+</sup> complexes when prepared in organic solvents; the polymeric [AgBr·MBI(acetone)<sub>0.5</sub>]<sub>4</sub> and the hexameric cluster [Ag·5MBI·THF]<sub>6</sub>. These complexes illustrate the importance of the counterion in the formation of the solid-state structure in reactions occurring within organic solvent based photothermographic image formulations. Since the carboxylate anion is a stronger conjugate base compared to halide, it is not surprising that the corresponding acid can readily form from deprotonation of the 5MBI while the AgBr reaction retains the halide. It is also worthwhile to revisit the presumed similarity of MBI reactivity relative to alkyl thioureas; considering the vast difference between the silver hexamer shown here and the Ag<sub>2</sub>S reported elsewhere, this presumption does not appear to be a good one.

In addition to MBI, there are many compounds within a standard photothermographic formulation that can act as silver complexing agents. We have now shown how two of these may compete for silver during the formulation, drying, and imaging processes, but this is just the beginning of what is required to better understand and improve these imaging materials.

## REFERENCES

- 1 T. H. James, *The Theory of the Photographic Process*, 4th ed. (Macmillan, New York, 1977).
- 2 T. Yokogawa, Japan Patent 01,100,177 (1989).
- 3 R. A. De Mauriac, Res. Discl. **150**, 18–21 (1976).

- <sup>4</sup>H. Daimatsu, Japan Patent 63,133,144 (1988).
- <sup>5</sup>H. Naito and M. Kato, Japan Patent 62,040,454 (1987).
- <sup>6</sup>H. Daimatsu, Japan Patent 62,040,446 (1987).
- <sup>7</sup>H. Kitaguchi and M. Kato, Japan Patent 61,067,851 (1986).
- <sup>8</sup>T. Masuda and S. Ikenoue, German Patent 2,433,292 (1976).
- <sup>9</sup>K. Okubo and T. Masuda, French Patent 1,567,962 (1971).
- <sup>10</sup>P. J. Cowdery-Corvan and D. R. Whitcomb, *Handbook of Imaging Materials*, edited by A. S. Diamond and D. S. Weiss (Marcel-Dekker, New York 2002), p. 473.
- <sup>11</sup>D. R. Whitcomb, "Photothermographic and thermographic imaging materials," *Kirk Othmer Encyclopedia of Chemical Technology* online edition 2002, <http://www.mrw.interscience.wiley.com/kirk/>
- <sup>12</sup>D. H. Klosterboer, *Imaging Materials and Processes, Neblette's*, 8th ed., edited by J. M. Sturge, V. Walworth, and A. Shepp (Van Nostrand-Reinhold, New York, 1989) Chap. 9, p. 279.
- <sup>13</sup>D. R. Whitcomb and R. D. Rogers, *J. Imaging Sci. Technol.* **43**, 504 (1999).
- <sup>14</sup>T. Tani, *Photograph. Sci. Eng.* **21**, 317 (1977).
- <sup>15</sup>T. Araki, K. Seki, S. Narioka, H. Ishii, Y. Takata, T. Yokoyama, T. Ohta, T. Okajima, S. Watanabe, and T. Tani, *Proc. 7th Int. Conf. X-Ray Abs. Fine Struct.*, *Jpn. J. Appl. Phys., Suppl.* **suppl. 32**(2), 815 (1993).
- <sup>16</sup>T. Hata, K. Tajima, and T. Mukaiyama, *Bull. Chem. Soc. Jpn.* **41**, 2746 (1968).
- <sup>17</sup>G. M. Sheldrick, *SHELXTL, version 5.05*, Seimens Analytical X-Ray Instruments Inc., 1996.
- <sup>18</sup>G. M. Sheldrick, *Program for Semiempirical Absorption Correction of Area Detector Data* (University of Göttingen, Germany, 1996).
- <sup>19</sup>S. Jablonka, C. Mora, P. M. Nowak, and A. Zaleski, *J. Inf. Rec.* **23**, 303 (1996).
- <sup>20</sup>P. M. Zavlin, A. N. Dyakonov, L. L. Kuznetsov, D. A. Efremov, and V. M. Belous, *Zh. Nauch. i. Priklad. Fotogr.* **41**, 66 (1996).
- <sup>21</sup>D. R. Whitcomb and R. D. Rogers, *J. Chem. Cryst.* **26**, 99 (1996).
- <sup>22</sup>G. Smith, D. E. Lynch, and C. J. L. Kennard, *Inorg. Chem.* **35**, 2711 (1996).
- <sup>23</sup>D. R. Whitcomb and M. Rajeswaran, *J. Imaging Sci. Technol.* **47**, 107 (2003).
- <sup>24</sup>M. Hong, W. Su, R. Cao, W. Zhang, and J. Lu, *Inorg. Chem.* **38**, 600 (1999).
- <sup>25</sup>L. Han, Z. Chen, J. Luo, M. Hong, and R. Cao, *Acta Crystallogr., Sect. E: Struct. Rep. Online* **E58**, m383 (2002).
- <sup>26</sup>P. A. Pérez-Lourido, J. A. Garcia-Vázquez, J. Romero, M. S. Louro, A. Sousa, Q. Chen, Y. Chang, and J. Zubieta, *J. Chem. Soc. Dalton Trans.* **1996**, 2047.
- <sup>27</sup>E. Block, M. Gernon, H. Kang, and J. Zubieta, *Angew. Chem., Int. Ed. Engl.*, **27**, 1342 (1988).
- <sup>28</sup>M. Shi, J.-K. Jiang, and G.-L. Zhao, *Eur. J. Inorg. Chem.*, **12**, 3264 (2002).
- <sup>29</sup>L. J. Ashfield, A. R. Cowley, J. R. Dilworth, and P. S. Donnelly, *Inorg. Chem.*, **43**, 4121 (2004).
- <sup>30</sup>K. Nomiya, S. Takahashi, and R. Noguchi, *J. Chem. Soc. Dalton Trans.* **2000**, 2091.